Conference Paper

A State-of-the-Art 3D Sensor for Robot Navigation

Author(s):
Weingarten, Jan W.; Gruener, Gabriel; Siegwart, Roland

Publication Date:
2004

Permanent Link:

https://doi.org/10.3929/ethz-a-010085479 →

A State-of-the-Art 3D Sensor for Robot Navigation

Jan W. Weingarten
Autonomous Systems Lab
Swiss Federal Institute of Technology (EPFL)
Lausanne, Switzerland
Email: jan.weingarten@epfl.ch

Gabriel Gruener
Swiss Center for Electronics
and Microtechnology (CSEM)
Alpnach, Switzerland
Email: gabriel.gruener@csem.ch

Roland Siegwart
Autonomous Systems Lab
Swiss Federal Inst. of Tech. (EPFL)
Lausanne, Switzerland

***Abstract*— This paper relates first experiences using a state-of-the-art, time-of-flight sensor that is able to deliver 3D images. The properties and capabilities of the sensor make it a potential powerful tool for applications within mobile robotics especially for real-time tasks, as the sensor features a frame rate of up to 30 frames per second. Its capabilities in terms of basic obstacle avoidance and local path-planning are evaluated and compared to the performance of a standard laser scanner.**

I. Introduction

Most mobile robot implementations until today rely on 2D sensors for creating maps, self localization, and collision avoidance. This is justified to some extent because most applications have been on ground robots, which inherently move in a 2D space.

The most widely used sensor is the laser range scanner, which provides a 180° view on the plane of measurement. Two such sensors can be mounted opposite to each other to provide a full planar view. Elaborate Simultaneous Localization and Mapping (SLAM) algorithms have been demonstrated using this sole sensor [10], [11]. Most systems use a horizontal laser scanner configuration, which has clear advantages for navigation but also clear drawbacks. The field of view of such a system is reduced to a single plane parallel to the floor, usually at knee height, neglecting indeed valuable information. In indoor environments typical examples are furniture (e.g. tables, chairs, cupboards), wall features (e.g. decorations, signalization, fire extinguishers), floor features (e.g. steps), etc.

Difficulties have been reported for collision avoidance [8] and during localization in *non-unique* situations [7]. To reliably avoid collisions a high number of additional sensors—usually ultrasound or infrared—are incorporated around the robot, adding robustness as well as complexity to the system—including additional sensor fusion algorithms [9]. Nevertheless, these additional sensors have a limited range of view and only produce one data value at a time—hence there is a need to have a plurality of them in order to produce denser data. Many environmental features can be identified by using stereo vision. Nonetheless, it lacks the ability to perceive unstructured surfaces which makes them less suitable for collision avoidance.

Recently, the Swiss Center for Electronics and Microtechnology (CSEM) has developed a new type of sensor called Swiss Ranger with the ability to produce dense three-dimensional data in real-time. In this paper we discuss our first experiences characterizing the sensor as well as its application for elementary collision avoidance in mobile robot navigation using a Dynamic Window Approach and the Vector Field Histogram. In order to qualify the results a parallel is drawn to a system using laser range scanners.

Section II describes the sensor and section III its characterization. The navigation algorithms used are discussed in section IV and the robot hardware and implementation in section V. Section VI shows the results obtained.

II. Sensor Description

The Swiss Ranger is a state-of-the-art, time-of-flight, solid-state imaging device that delivers distances as well as gray-level (i.e. intensity) images developed by CSEM [1]. It has been demonstrated that for a large range of illumination levels the range accuracy is essentially only limited by the shot noise of the available light [2]. This allows to predict reliably the obtainable range resolution. In other words, for every measurement there is a reliable prediction of its resolution, which is necessary for state-of-the-art robot navigation.

A. Measurement Principle

The camera is based on a 2-dimensional dedicated image sensor and a modulated light source. Every pixel on the sensor samples the amount of modulated light reflected by objects in the scene. This is done four times every period at equal intervals (see Fig. 1). Let us name these measurements m_1 to m_4. These four quantities allow to recover the sinusoidal incoming signal. The phase shift between the emitted light and the returning signal is:

$$\varphi = \arctan\left(\frac{m_4 - m_2}{m_1 - m_3}\right) \tag{1}$$

and determines the distance to the objects in the scene:

$$L = L_{max}\frac{\varphi}{2\pi} \tag{2}$$

L_{max} is the non-ambiguity range of the sensor, determined by the modulation frequency of the emitted light. The

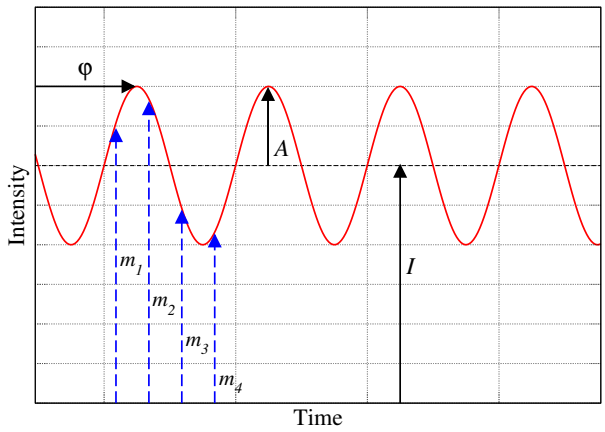

Fig. 1. Measurement principle of the Swiss Ranger. Four intensity measurements (m_i) done at equal intervals each period allow to recover the measured modulated sinusoidal: the phase shift φ, the average intensity I, and the amplitude A.

intensity of the objects in the image is recovered from the average light reflected:

$$I = \frac{m_1 + m_2 + m_3 + m_4}{4} \tag{3}$$

The amplitude of the measured sinusoidal:

$$A = \frac{\sqrt{(m_3 - m_1)^2 + (m_4 - m_2)^2}}{2} \tag{4}$$

allows to predict the quality of the measurement:

$$\Delta L = \frac{L_{max}}{\sqrt{8}} \frac{\sqrt{I}}{2A} \tag{5}$$

B. Implementation

The Swiss Ranger's image sensor has been implemented on 0.8 μm CMOS / BCCD technology. It contains 160 by 124 pixels, each pixel being 39.2 μm wide by 54.8 μm high. The emitted light modulation frequency is typically 20 MHz, yielding a non-ambiguity range of 7.5 m. The modulated illumination is generated by a set of 48 near-infrared LEDs. The field of view (fov) depends on the lense used, which in our case is about $43°$ (horizontally) and $46°$ (vertically), implying an angular resolution of $0.35°$ in the worst case. Figure 2 shows the Swiss Ranger in its latest configuration. Note that the sensor contains no moving parts.

The current configuration of the camera is available as an evaluation prototype. It includes an FPGA that recovers the data from the sensor and applies equations (1) to (4). A USB interface is used to talk with the camera from a client. After the client requests a picture, an array of pixels representing the measured (and calculated) distance and intensity is returned. Several parameters can be adjusted by the client through the USB interface, like L_{max}, data filtering by amplitude threshold, etc. Note that in its current implementation, the FPGA does not include a mode that allows the client to recover the raw measurements m_i. Figure 3 shows a typical measurement of the sensor in an office environment.

Fig. 2. The time-of-flight Swiss Ranger sensor from CSEM. Note that sensor contains no moving parts.

In order to understand better the capabilities of the Swiss Ranger, it makes sense to compare it, in the context of Mobile Robotics, with the preferred sensor used at this moment by the community: the laser range scanner. Table I lists briefly some of the key characteristics of both sensors.

TABLE I
CHARACTERISTICS OF THE SWISS RANGER AND A TYPICAL LASER RANGE SCANNER

Characteristic		CSEM Swiss Ranger[a]	SICK LMS 200
Range [m]		7.5	25
Accuracy [mm]		5[b]	10
Horizontal fov [°]		43	180
Vertical fov [°]		46	0
Angular resolution [°] (best / worst)		0.28 / 0.35	0.25 / 1.0
Distance data points		19840	361
Intensity data points		19840	reflectivity data[c]
Measurement quality		Yes each pixel	No
Speed [fps]		30	50
Interface		USB 2 (480 Mb/s)	RS422 (500 kb/s)
Weight [kg]		0.3	4.5
Size	width [m]	0.145	0.155
	depth [m]	0.032	0.156
	height [m]	0.04	0.21
Energy consumption [W]		12	20
Price [USD]		7700.-	5700.-

[a] Evaluation prototype
[b] Average for one pixel
[c] Mainly used for on / off beacon extraction

III. CHARACTERIZATION

First tests done with an evaluation prototype of the Swiss Ranger have shown that there is a tangible amount of irregularities in the generated data. This is due to a

certain mismatch within each pixel because a so-called 2-tap pixel architecture is used. The effect becomes more pronounced toward the edges of the sensor. A 1-tap pixel configuration could be used, which would eliminate most noise and irregularities while cutting the frame rate by half [3]. This section analyzes these effects and proposes a way to compensate them by preprocessing the data.

A. Calibration using intensity information

As the Swiss Ranger disposes of a standard optical lens to capture the reflected light, it needs to be calibrated just like a standard video camera in order to get rid of distortions and misalignments of the optical axis of the lens and the sensor. This was achieved by using the freely available "Calibration Toolbox for Matlab", which is based on [12] and [13]. It makes use of the pinhole camera model and requires several images from different viewpoints of a checkerboard calibration object with known dimensions.

The found focal length of $f = 8.06$ mm corresponds well to the manufacturer's specification of 8 mm. The misalignment of the optical axis of the lens and the center of the CCD sensor amounts to a non-negligible 3.4mm in the horizontal axis and 3.5mm in the vertical axis .

B. Calibration using range information

A test environment using a planar wall[1] located at a fixed distance (1.4 m) perpendicular to the optical axis of the sensor was used to perform the tests. While this is certainly not representative for all measurement situations, it has the advantage that the ground truth represented by a wall is precisely known and only depends on the distance from the sensor.

1) Distance Calibration: As described above, the sensor performs a time-of-flight measurement which detects a phase shift in the modulated emitted signal (1) which can in turn be translated into a distance (2). In practice, due to propagation delay in the driving circuits of the camera, a distance offset has to be included[2]. The offset is determined experimentally during calibration and can be set by the user on the Swiss Ranger configuration registers.

The precision of the sensor can be quantified by comparing the distance measured by the Swiss Ranger with the ground truth for several distances. Using a planar surface for calibration simplifies this process, since the expected range can be easily calculated for all 19840 pixels. It was observed that the distance vs. phase offset relation did not hold, as (2) models: calibrating the offset with a close-by reference wall would not hold for far references. Nevertheless, let us remember that the actual raw data is the 4 m_i discussed above. A direct calibration would be based on these quantities and not on the results of (1) and (2). Nonetheless, our evaluation prototype delivered only distance and intensity directly. In order to callibrate the distance measurement under the given conditions, the following empirical relation is proposed:

$$L = k(L_{max}\frac{\varphi}{2\pi} + L_0) \tag{6}$$

where L_0 is the distance offset and k is a linearization factor. Through calibration the following values were found: $L_0 = 0.6$ m, $k = 1.18$.

2) Accuracy: To get an idea of the statistical spread of a typical data set taken in a real office environment, one hundred consecutive measurements were performed on the same reference surface The resulting standard deviation, averaged over all 19840 pixels, is $\sigma = 0.024$ m. Note that only the accuracy in the direction of the received light beams is considered, which changes with varying distances, used materials, etc. Also note that this definition of accuracy (averaged over all pixels) differs from the camera's specifications, which are done for one pixel alone.

C. Data Preprocessing

The above effects have to be taken into account to the extent that a particular application requires. In the case of obstacle avoidance and path planning for a mobile robot, high certainty is preferred: a measured data point should closely match an object in the real world and vice versa. Otherwise it would be impossible to guarantee safe operation of the robot.

As a first step, the uncertainty value generated by the sensor as a function of measured amplitude (4) is used to filter out inaccurate data points. In addition, a simple grid-based filtering method was implemented. A regular grid defined around the pyramidal viewing range of the sensor is used to decompose the space into cells. Each cell must contain a minimum number of data points to be considered occupied. This number is found empirically and depends on the cell size and on the corresponding measured distance, since data density decreases with increasing distance. This method provides an effective filter while reducing the amount of data available lending itself particularly well for grid-based collision avoidance and path planning algorithms.

IV. Application: Mobile Robot Navigation

In order to evaluate the Swiss Ranger sensor on an actual mobile robotic application, a navigation system was implemented. The system consists of a lower-level reactive collision avoidance scheme implemented with a Dynamic Window Approach and an upper-level path planning scheme based loosely on a Vector Field Histogram. The goal was to quickly accomplish a simple, functional navigation system that would allow to test the capabilities of the Swiss Ranger.

A. Dynamic Window Approach

A Dynamic Window Approach (DWA) [4] is used for collision avoidance during navigation. The DWA generates actuator commands such that the robot does not collide with obstacles and the commands do not violate the dynamic capabilities of the robot. In this way, it assures that no collisions will happen irrespective of the speed of the robot. An existing DWA implementation in our laboratory

[1] Of a flat, painted, metallic material with a slightly increased reflectivity in the orange color

[2] A delay of 1 ns already implies an offset of about 0.15 m

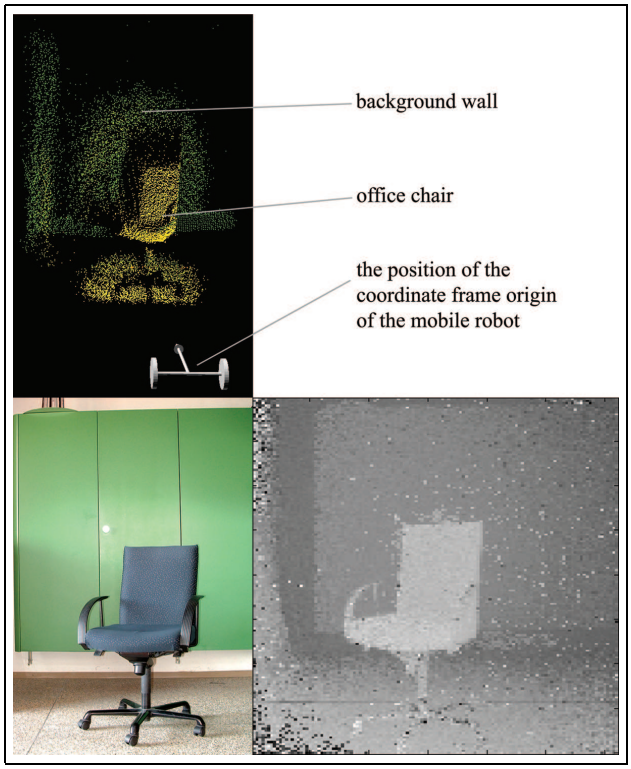

Fig. 3. Sample Swiss Ranger measurement (bottom right), color coded for distance. An office chair (see photograph bottom left) is seen in the middle of the image and closer to the sensor. The top left image shows the same scene converted into cartesian coordinates.

was used [5], which uses a freely definable robot shape and pre-calculated lookup tables for fast collision prediction.

The DWA requires a local grid that maps sensed obstacles into occupancy cells. Cell occupancy can be quickly generated after the data from the Swiss Ranger is filtered as described above. The algorithm uses a fresh grid at each processing step (i.e. no previous measurements are stored).

B. Vector Field Histogram Path Planning

The DWA requires intermediate goal points as input. These goal points are generated by a Path Planner. An adapted Vector Field Histogram (VFH) [6] is used due to its simplicity, computational efficiency, and robustness. It uses an angular histogram containing vector field information generated by repulsing obstacles around the robot and finds travel-safe angular sectors for local path-planning. The histogram is built using weighted proximity information in the local occupancy grid, closer objects being more significant. Free sectors are quickly found by thresholding and the one closest to the goal's heading is chosen to generate an intermediate goal.

In theory, a VFH uses a 360° view of the environment. This can be accomplished with 2 opposing laser range scanners or by using a panoramic array of one-dimensional sensors like ultrasonic or infrared sensors. In the case of the Swiss Ranger, this could be done by mounting several sensors around the robot. In our case, though, we had only one evaluation prototype. It became relevant—due to the limited field of view—to incorporate a sense of memory so that obstacles that fall out of view due to a robot movement are not immediately forgotten. This was done by generating a transient local map that registers the data points based on odometry. The procedure assumes, though, a static environment, which suffices for our purposes.

V. Implementation

A. Hardware

The robot used for this study is shown in Figure 4. It is a differential-drive mobile robot equipped with a multitude of sensors: two opposing horizontal SICK LMS 200 laser range scanners for a field of view of 360°, four ultrasound, and five infrared distance sensors; and a 1000 Hz odometry controller. Two computers—a PowerPC 750 (400 MHz) running the hard RTOS XO/2 and a Pentium III (700 MHz) running Microsoft Windows 2000—are available to control the robot and process data. In this work, only the PowerPC to control the robot motion was used. External communication with the robot is done through an Ethernet or WLAN connection.

The Swiss Ranger was mounted on the front side of the robot without occluding the field of view of the laser range scanners. This enabled alternate or simultaneous use of the sensors. An external laptop computer processed sensor and odometry information and generated motion commands. Note that neither the ultrasound nor the infrared sensors were used.

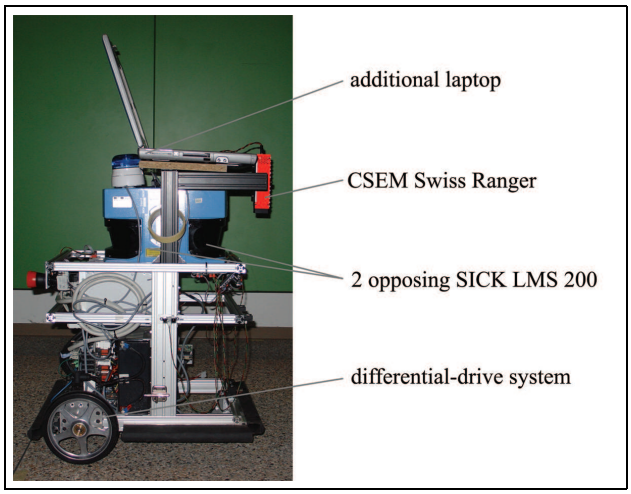

Fig. 4. The mobile robot used with two opposing SICK LMS 200 sensors and a CSEM Swiss Ranger in front.

B. Software

The visualization software developed is based on the Visualization Toolkit (VTK)—a freely available scientific visualization package using the OpenGL graphics standard.

The implementation aimed at being capable of easily switching between the laser scanners and the Swiss Ranger. Since the latter produces 3D data but the DWA as well as the VFH approach use 2D data, the 3D data was merged. In this first implementation, the 3D data was simply squeezed into a 2D grid from the top down. Data points at locations higher than the robot top were not included. In this way,

tables, for example, appear occupying a whole rectangular area in the grid. This differs from grids commonly generated by laser scanners, which would mark only the cells at the table's legs as occupied.

VI. Experimental Results

This section presents the accomplished experiments with acquired results. All experiments were carried out twice, once with a standard laser scanner and another time with the Swiss Ranger.

A. Collision Avoidance with DWA

In a first simple experiment, the robot had to move on a straight line towards a solid obstacle, the overall goal lying beneath it. The local path-planner using the VFH approach was turned off. The laser scanner was chosen to start with and the result was as expected, the robot stopped shortly in front of the obstacle. The same experiment was carried out using the Swiss Ranger and the result was the same. The Dynamic Window Approach therefore seemed to work adequately with either sensor.

The second test case was more difficult because the solid obstacle was substituted by a table (See Fig. 5). Since the table top did not lie at the same height as the scanning plane of the laser scanners, it was not seen and therefore lead the robot to a collision. Using the Swiss Ranger prevents the robot from colliding, as the table easily falls into the vertical field of view of the sensor. The resulting robot path visualization is shown in Figure 6.

Fig. 5. Test case 2: A table blocks a corridor and the robot's path.

B. Local Path-Planning

Test case 3 involved the local path-planner using the Vector Force Histogram approach. The robot had to move through a doorway and avoid a wall (see Fig. 7). The results are shown in Figure 8. It can be observed that both sensors lead the robot successfully to the goal. When using the laser scanners, given their wider field of view, they are able to extract data representing the open door on the right. This

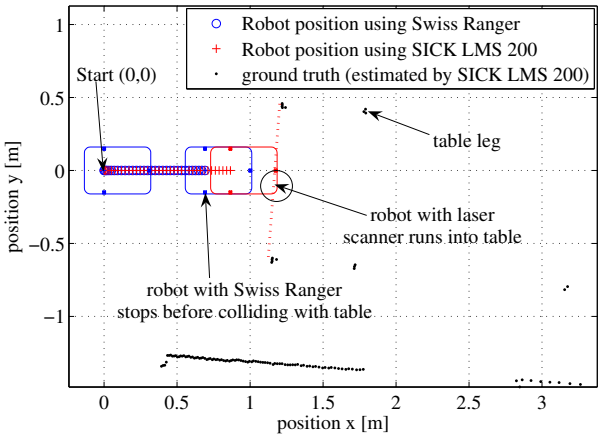

Fig. 6. Trajectories of the robot for test case 2: The laser scanners fail to detect the obstacle and a collision ensues. The Swiss Ranger detects the obstacle and the collision is avoided.

leads to a slightly different path than the path generated using the Swiss Ranger which due to its narrower field of view does not extract the door. This result shows that the Swiss Ranger can not only be used for collision avoidance but at least also for simple path-planning tasks.

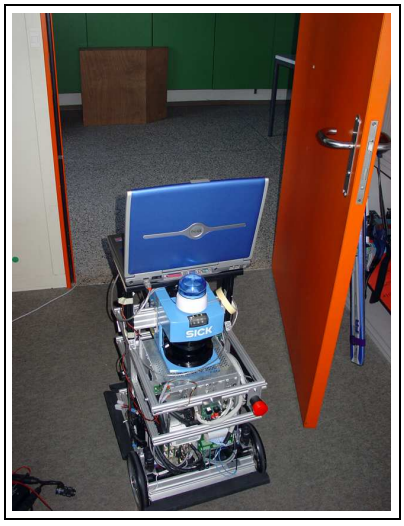

Fig. 7. Test case 3: Driving through a door way.

VII. Conclusion

A state-of-the-art time-of-flight range sensor has been presented and characterized. The sensor was used for basic navigation of a mobile robot. A comparison has been drawn with a laser range scanner. The key advantages of the Swiss Ranger are its ability to generate real 3D range as well as intensity data at high speed in an all-solid-state, compact, and light package. The results are promising. Future work will study the use of the Swiss Ranger for other mobile robotics tasks, like 3D mapping and localization.

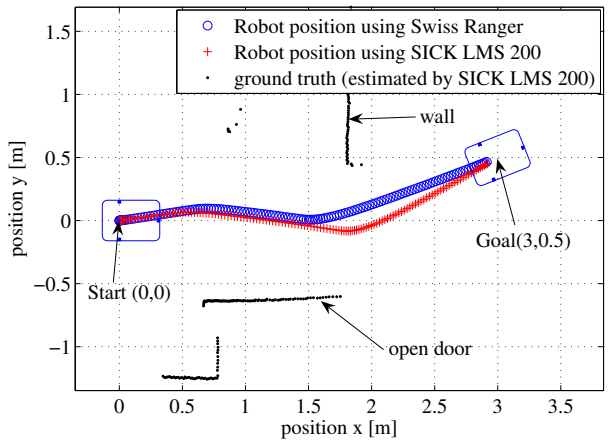

Fig. 8. Trajectory of the robot for test case 3: The wider field of view of the laser scanners incorporates data from the open door on the right, yielding a path parallel to the doorway. The narrower field of view of the Swiss Ranger fails to see the door and a smoother path is followed. Note that both trajectories detect the doorway correctly and reach the goal point equally.

ACKNOWLEDGMENTS

The authors would like to thank Thierry Oggier for his support with the Swiss Ranger evaluation prototype and Roland Philippsen for his support with the Dynamic Window Approach implementation. This work was funded by a CSEM research grant.

REFERENCES

[1] R. Lange and P. Seitz, “Solid-State, Time-of-Flight Range Camera”, *IEEE Journal of Quantum Electronics*, 2001, v. 37, n. 3, pp. 390-397.

[2] T. Oggier, M. Lehmann, R. Kaufmann, M. Schweizer, M. Richter, P. Metzler, G. Lang, F. Lustenberger, N. Blanc, “An all-solid-state optical range camera for 3D real-time imaging with sub-centimeter depth resolution (SwissRanger)”, *SPIE Optical Design and Engineering*, St. Etienne, France, February 2004, v. 5249, pp. 534-545.

[3] R. Kaufmann, M. Lehmann, M. Schweizer, M. Richter, P. Metzler, G. Lang, T. Oggier, N. Blanc, P. Seitz, G. Gruener, U. Zbinden, “A Time-of-Flight Line Sensor - Development and Application”, *Proceedings of the SPIE Photonics Europe Conference 5459-23*, Strasbourg, France, April 2004.

[4] D. Fox, W. Burgard, S. Thrun, “The Dynamic Window Approach to Collision Avoidance”, *IEEE Robotics & Automation Magazine*, March 1997, v. 4, n. 1, pp. 22-33.

[5] R. Philippsen and R. Siegwart, “Smooth and Efficient Obstacle Avoidance for a Tour Guide Robot”, *Proceedings of the IEEE International Conference on Robotics and Automation*, 2003, Taipei, Taiwan, pp. 446-451.

[6] J. Borenstein, Y. Koren, “The Vector Field Histogram - Fast Obstacle Avoidance For Mobile Robots”, *IEEE Journal of Robotics and Automation*, 1991, v. 7, n. 3, pp. 278-288.

[7] K.O. Arras , J.A. Castellanos, M. Schilt and R. Siegwart, “Feature-based multi-hypothesis localization and tracking using geometric constraints”, *Elsevier, Robotics and Autonomous Systems*, 2003, v. 1056, pp. 1-13.

[8] B. Jensen, G. Ramel and R. Siegwart, “Detecting Semi-Static Objects with a Laser Scanner”, *Proceedings of Autonome Mobile Systeme*, 2003, Karlsruhe.

[9] T.S. Jin, J.M. Lee, “Abstract Mobile Robot Navigation Used Space and Time Sensor Fusion In an Unknown Environment”, *Proceedings of the International Conference on Intelligent Robots and Systems*, October 2002, Lausanne, pp. 613-618.

[10] S. Thrun, M. Beetz, M. Bennewitz, W. Burgard, A.B. Cremers, F. Dellaert, D. Fox, D. Hähnel, C. Rosenberg, N. Roy, J.Schulte, D. Schulz, ”Probabilistic Algorithms and the Interactive Museum Tour-Guide Robot Minerva”, *Journal of Robotics Research*, 2000, v. 19, n. 11, pp. 972-999.

[11] J.E. Guivant, E.M. Nebot, ”Optimization of the simultaneous localization and map-building algorithm for real-time implementation”, *IEEE Transactions on Robotics and Automation*, 2001, v. 17 , n. 3, pp. 242-257.

[12] Z. Zhang, ”Flexible Camera Calibration By Viewing a Plane From Unknown Orientations”, *The Proceedings of the Seventh IEEE International Conference on Computer Vision*, 1999, Kerkyra, v. 1, pp. 666-673.

[13] J. Heikkilä, O. Silvén, ”A Four-step Camera Calibration Procedure with Implicit Image Correction”, *Proceedings of Computer Vision and Pattern Recognition*, 1997, San Juan, pp. 1106-1112.